12th International Conference on Applications of Statistics and Probability in Civil Engineering, ICASP12
Vancouver, Canada, July 12-15, 2015

Integrated Multi-Hazard Framework for the Fragility Analysis of Roadway Bridges

Pierre Gehl
Research Associate, EPICentre, Dept. of Civil Engineering, University College London, London, UK

Dina D'Ayala
Professor, EPICentre, Dept. of Civil Engineering, University College London, London, UK

ABSTRACT: This paper presents a method for the development of bridge fragility functions that are able to account for the cumulated impact of different hazard types, namely earthquakes, ground failures and fluvial floods. After identifying which loading mechanisms are affecting which bridge components, specific damage-dependent component fragility curves are derived. The definition of the global damage states at system level through a fault-tree analysis is coupled with a Bayesian Network formulation in order to account for the correlation structure between failure events. Fragility functions for four system damage states are finally derived as a function of flow discharge Q (for floods) and peak ground acceleration PGA (for earthquakes and ground failures): the results are able to represent specific failure configurations that can be linked to functionality levels or repair durations.

1. INTRODUCTION

Spatially distributed infrastructure networks may be exposed to a wide range of natural hazards, whose impacts have to be integrated and homogenized in order to assess the reliability of the system over the design lifetime of its components (e.g. roadway bridges). While previous studies have proposed probabilistic frameworks for multi-hazard assessment, either for joint independent events or cascading events (Marzocchi et al., 2012), there remains a lack of fragility models that are able to account for hazard interactions at the vulnerability level. Even though some vulnerability analyses have addressed the combined effects of earthquakes and scour (Alipour and Shafei, 2012) or earthquakes, scour and truck traffic on bridges (Liang and Lee, 2013), integrated fragility functions with respect to the various intensity measures that represent the hazard types are needed in order to be coupled to the probabilistic hazard distributions.

To this end, a component-based approach is proposed in this paper: the bridge system is decomposed into its various components, so that the hazard-specific loading mechanisms and their demand can be straightforwardly quantified at the component level. In the case where some damaged components influence the response of other components with respect to another hazard types, a set of damage-dependent component fragility curves have to be derived in order to account for all possible damage configurations. Finally, the use of probabilistic tools such as Bayesian Networks can facilitate the assembly of the component fragility curves at system level, while accounting for the possible correlations between the component failure events. Multi-variate fragility functions are then expected to be derived, where each input variable represents a hazard-specific intensity measure, so that the damage of the bridge system can be assessed for joint hazard events as well as single events.

2. MULTI-HAZARD SCENARIOS

Three main hazard types are considered in the present study, namely earthquakes (EQ), fluvial floods (FL) and earthquake-triggered ground failures (GF). They have been chosen because they may affect a wide range of bridge components and they are among the main causes of bridge failures (Sharma and Mohan, 2011).

Following the classification proposed by Lee and Sternberg (2008), different types of multi-hazard scenarios have to be considered:

- Simple events: for instance, EQ, FL or GF events taken separately (Scenario 1).
- Combined multi-hazard events (i.e. a single event triggering multiple loading mechanisms): a GF event triggered by an EQ event (Scenario 2).
- Subsequent multi-hazard events (i.e. unrelated single events separated in time): it could be a FL event followed by an EQ, which in turn triggers a GF event (Scenario 3).
- Simultaneous multi-hazard events: they represent the most unlikely scenarios and are not addressed here.

These different scenarios are then considered throughout the rest of the paper, as the objective is to generate multi-hazard fragility curves that are able to account for different combinations of loading mechanisms.

3. BRIDGE COMPONENTS AND ASSOCIATED FAILURE MECHANISMS

A multi-span concrete bridge with simply-supported independent decks is considered in the present study. It is composed of two seat-type abutments and two piers with three cylindrical RC columns. Deck displacement is restrained by elastomeric bearings (i.e. alternation of expansion and fixed devices) in the longitudinal direction and shear keys in the transversal direction. At each bridge extremity, an embankment approach is added in order to simulate the transition between the plain roadway segment and the bridge (see half bridge system in Figure 1).

The hazard types that may potentially affect the various bridge components are detailed in Table 1:

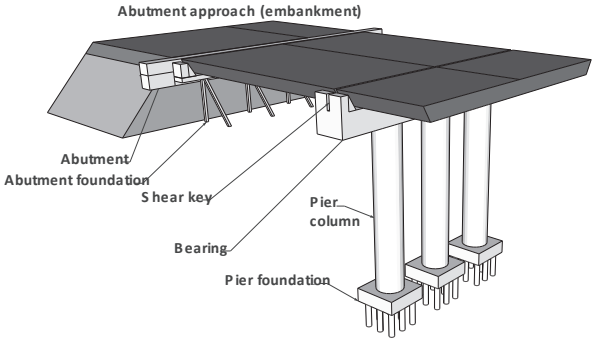

Figure 1: Sketch of the studied bridge system and its components.

- Earthquakes affect all structural components of the bridge (i.e. abutments, piers, bearings, shear keys).
- Fluvial floods may excavate pier foundations due to scour, while in extreme cases decks may be dislodged by hydraulic forces, after shear keys have been damaged (Padgett et al., 2008).
- Earthquake-triggered ground failures are likely to affect the approach embankment, as there is usually a vertical settlement between the embankment and the bridge, due to the difference in foundation depth (Puppala et al., 2009). Deep-seated landslides may also affect the slope on which the abutment is built.

Table 1: Bridge components and associated hazard types.

Component	EQ	FL	GF
Pier foundation		X	
Pier	X		
Bearing	X		
Deck		X	
Abutment foundation			X
Abutment	X		
Abutment approach			X
Shear key	X	X	

4. COMPONENT FRAGILITY CURVES

Fragility models are derived to quantify the damage probability of each component to their associated hazard types.

4.1. Earthquake

The layout, dimensions and constitutive models of the different bridge components are directly taken from the multi-span simply-supported concrete (MSSSC) girder bridge described in the study by Nielson (2005). However two modifications are brought to the bridge system:

1. Pier foundations are assumed to be anchored up to a depth of 8 m: the group of pile foundations, as described by Nielson (2005), is approximated by an equivalent elastic beam, which is connected to the ground through a set of Winkler *p-y* springs in order to model the soil resistance. The bending stiffness of the equivalent pile and the parameters of the *p-y* curves are based on the configuration of the group piles and the soil properties (Prasad and Banerjee, 2013).
2. External shear keys are added on the pier caps in order to restrain the displacement of the independent decks in the transversal direction. The shear keys are modelled according to a sliding friction shear mechanism: first, the deck can slide on the pier cap (i.e. friction Coulomb law) until the gap with the shear key is closed. Then, the capacity of the shear key is engaged until it ruptures through a shear mechanism. Once the shear key has failed, it is assumed that the deck can slide again until unseating.

The bridge is modelled through a simplified system of connectors whose stiffness and hysteretic models represent the behaviour of the different bridge components, such as piers, bearings or abutments (Gehl and D'Ayala, 2014). For instance, each three-column pier is fully modelled with a finite element program and its cyclic pushover curve in both longitudinal and transversal directions is then used to model an hysteretic material spring in the OpenSees platform.

Following the multi-hazard scenarios defined in the previous section, the seismic fragility curves should be derived for various configurations:

- Intact bridge;
- Pier foundations excavated by scour;
- Shear keys damaged by hydraulic forces (i.e. fluvial flood);
- Both pier foundations and shear keys affected by a fluvial flood.

Therefore the bridge response has to be reassessed for each of the identified configurations, leading to a series of damage-dependent component fragility functions. The effect of scour is introduced by removing the Winkler springs that are excavated by the scour depth (Alipour et al., 2013). If damaged, shear keys are simply removed and the transversal deck movement is only restrained by a friction law.

Fragility curves for each component, for both loading directions, and for two damage states (i.e. yield and collapse for piers and abutments; restraint failure and unseating for bearings and shear keys) are then derived using the limit states defined in Nielson (2005): non-linear dynamic analyses on the simplified bridge model are carried out with 288 synthetic records for an appropriate range of magnitude and epicentral distance (see Gehl and D'Ayala (2014) for more details). In the longitudinal direction, 10 components are considered (i.e. piers P1 and P2, abutments Ab1 and Ab2, fixed and expansion bearings B1 to B6), as well as in the transversal direction, except that the bearings are then replaced by the shear keys.

Fragility curves have been derived for different scour depths (i.e. from 0 to 5.1 m): based on the evolution of the bridge response and the fragility parameters, three threshold levels of scour depth have been identified: starting from 1 m, some changes in the bridge response can be observed (i.e. scour damage state D1); from 3.6 m, the behaviour of the pier changes dramatically and the effect of scour is much more noticeable (D2); finally, it is assumed that, after 5.1 m, the pier has almost a pinned connection to the soil and the stability of the system cannot be guaranteed (D3).

From Figure 2 it can be observed that scour has mainly a detrimental effect on the bearings, which tend to fail earlier as scour depth increases. Since the pier connection is relaxed at their base, they experience lower bending moments and their failure probability decreases for higher scour levels (however shear failure is not currently modelled). Finally, the response of abutments seems to remain

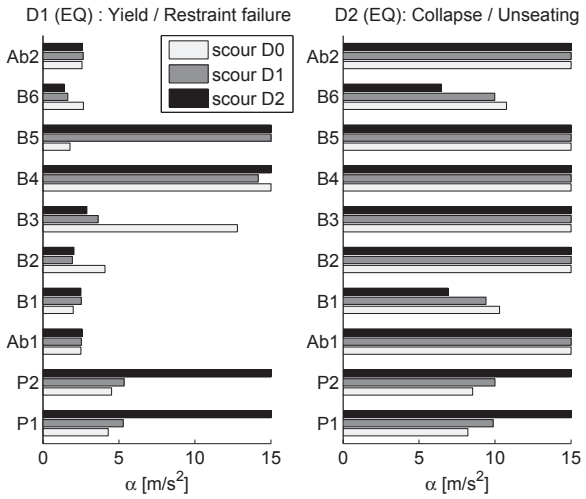

Figure 2: Mean fragility parameter α in the longitudinal direction, for the different components and their two damage states, for different initial states of scour damage.

stable across the different scour depth. Similar observations have been made when fragility curves are computed in the transversal direction.

The effect of previous shear key failure is only observed for fragility curves in the transversal direction: the influence of shear keys is not significant for lower damage states (i.e. yield), however the absence of shear keys leads to a much earlier occurrence of heavier damage states, especially deck unseating.

4.2. Ground failure

As discussed in the previous section, earthquake-triggered ground failures are more likely to affect the components that are located at the bridge extremities, namely the approach embankment and the abutment foundations. First, the fragility of approach embankments with respect to lateral spreading of the supporting soil is taken from Kaynia et al. (2012). Using the first two damage states (i.e. slight damage D1 with permanent ground displacement of 3 cm and moderate D2 with permanent ground displacement of 15 cm), fragility parameters for D1 (respectively D2) are the mean $\alpha_1 = 1.96$ m/s^2 (resp. $\alpha_2 = 4.12$ m/s^2) and the standard deviation $\beta_1 = 0.70$ (resp. $\beta_2 = 0.70$), for a European soil type D and an embankment height of 2 m.

Regarding the abutments, their deep foundations prevent the occurrence of damage due to superficial landslides with a planar sliding surface: however the damage due to a deep-seated circular landslide that occurs below the foundations may have to be considered. In this case, the factor of safety FS is estimated with the limit equilibrium method (i.e. Bishop's simplified method), assuming a circular slip surface (see Figure 3). The surface is subdivided into a number n of vertical slices and the factor of safety FS is then expressed as the ratio of resisting versus destabilizing moments of all the slices.

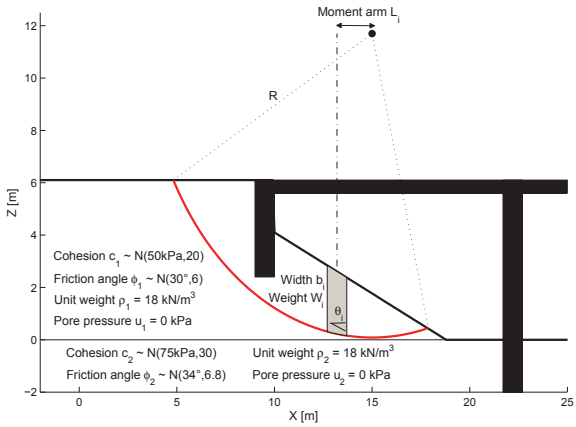

Figure 3: Slice equilibrium method for the estimation of the factor of safety. The black shape is a simplified view of the studied bridge and its foundations.

Fragility functions for slope instability (D1) are then derived following the method proposed by Wu (2014): for each increasing value of PGA, the reliability index of $\ln FS > 0$ is estimated using a Mean-Value First-Order Second Moment (MFOSM) method. The input random variables are the cohesion and friction angle of each soil layer, while a correlation factor of -0.4 is assumed between the cohesion and the friction angle (Wu, 2013). The search algorithm for the probabilistic critical surfaces proposed by Hassan and Wolff (1999) is used in order to ensure that the minimum reliability index is found for each combination of the soil parameters, which is different that finding the surface with the smallest factor of safety. An additional constraint is introduced by the location of the abutment and pied foundations, since the crit-

ical surface is unlikely to generate any failures if it intersects with the bridge foundations. Finally, the reliability index is converted into the probability of failure P_f and the points $\mathrm{PGA} - P_f$ are fitted into a fragility curve with a lognormal cumulative distribution function: a mean of 12.62 $\mathrm{m/s^2}$ and a standard deviation of 1.03 have been found.

4.3. Scour

For the purpose of the demonstration, only local scour at piers is considered, since it could be assumed that there is no contraction of the river bed cross-section. Also, general scour due to river bed degradation is usually neglected with respect to local scour. Empirical equations from HEC-18 (Richardson and Davis, 1995) are used to quantify the excavated depth y_s due to local scour at piers:

$$y_s = 2 \cdot K_1 \cdot K_2 \cdot K_3 \cdot K_4 \cdot y \cdot \left(\frac{D}{y}\right)^{0.65} \cdot F^{0.43} \quad (1)$$

Where y represents the flow height, D is the pier width, F is the Froude number and the K_i parameters are corrective coefficients (see Table 2). Finally, the flow discharge Q can be expressed as a function of velocity v and height y (Alipour et al., 2013), with river section width b:

$$Q = b \cdot y \cdot v = \frac{b \cdot y}{n} \cdot \left(\frac{b \cdot y}{b + 2y}\right)^{2/3} \cdot S_0^{1/2} \quad (2)$$

The Manning's roughness coefficient n and slope grade S_0 are specified in Table 2.

Based on the probabilistic distribution of the input parameters, a Monte Carlo scheme is used with sampled values of flow height y in order to generate around 10,000 couples of points $Q - y_s$, which are related by the combination of Equations 1 and 2. This data set is then used to generate fragility curves with respect to flow discharge Q, using the three scour depth thresholds that have been previously defined. A comparative analysis of different statistical models has shown that the lognormal cumulative distribution function is the best fit for these scour fragility curves. The derived fragility parameters for damage states D1, D2 and D3 are means $\alpha_1 = 2.74$ $\mathrm{m^3/s}$, $\alpha_2 = 285.77$ $\mathrm{m^3/s}$, $\alpha_3 = 847.62$ $\mathrm{m^3/s}$ and standard deviations $\beta_1 = 0.55$, $\beta_2 = 0.57$ and $\beta_3 = 0.53$.

Table 2: Values used in the scour equations. Some of the parameter distributions are taken from Alipour and Shafei (2012).

Variable	Description	Distribution
K_1	Factor for pier nose shape	$K_1 = 1$
K_2	Factor for flow angle of attack	$\mathscr{U}(1, 1.5)$
K_3	Factor for bed condition	$\mathscr{N}\left(1.1, 0.055^2\right)$
K_4	Factor for bed material size	$K_4 = 1$
n	Manning's roughness coefficient	$\ln\mathscr{N}\left(0.025, 0.275^2\right)$
S_0	Slope grade	$\ln\mathscr{N}\left(0.02, 0.5^2\right)$

4.4. Submersion

While several studies have dealt with the vulnerability of bridges due to hurricanes and related storm surges (Kameshwar and Padgett, 2014; Padgett et al., 2008), the impact of fluvial floods on bridge superstructures remains difficult to quantify. Therefore, as a very raw approximation and for the sake of the demonstration, the fragility curve from Kameshwar and Padgett (2014) for bridge failure due to storm surge is taken in order to represent the probability of deck unseating (D2), while keeping the coefficient related to wave height equal to 0.

Regarding damage to shear keys (D1), a conservative assumption could consist in considering failure as soon as the flow height reaches the top of the pier cap. These threshold values can then be converted in terms of flow discharge using Equation 2.

5. GLOBAL DAMAGE STATES

Global damage states should be defined so that they are consistent in terms of gravity of damage and consequences on the bridge functionality. Therefore a rationale is proposed here in order to identify homogeneous system damage states (SDSs) depending on all possible combinations of component damage states, based on the functionality level of the bridge and the repair operations

required:

- SDS1 (slight repairs and no closing time): slight damage to approach embankments (D1) without a significant impact on the bridge functionality, even though repair operations are eventually necessary;
- SDS2 (moderate repairs and short closing time): structural damage to bridge components (i.e. piers, abutments, bearings and shear keys in damage state D1 due to earthquake, approach embankments in damage state D2 due to ground failure, damaged shear keys D1 due to flood);
- SDS3 (extensive repairs and closing time): deck unseating that induces long term closure of the bridge, even though temporary deck spans could be installed if the substructure components have not collapsed (i.e. deck unseating D2 due to flood, bearings and shear keys in damage state D2 due to earthquake);
- SDS4 (irreparable with full collapse): substructure components have collapsed and induce the total failure of the bridge system (i.e. piers and abutments in damage state D2 due to earthquake, scour damage state D3 at pier foundations, slope failure D1 beneath abutment foundations).

These system damage states can be represented through a fault-tree analysis, as shown by the example in Figure 4, where the cascading failures leading to the global failure event can be detailed: the seismic response of all bridge components is dependent on the foundations conditions, therefore the failure events of bearings and shear keys (i.e. $B_{EQ,2}$ and $Sh_{EQ,2}$) should also be expressed as a function of the damaged pier foundations due to floor/scour ($Pf_{FL,i}$ representing the different scour damage states). For each scour damage state, the bearing failure events are differentiated into specific events $B^{\circ}_{EQ,2}$, $B'_{EQ,2}$ and $B''_{EQ,2}$, in order to represent the different failure probabilities for different scour levels (see Figure 2). The same development has to be applied to the $Sh_{EQ,2}$ event, which also has to account for the likelihood of having the shear keys previously damaged by flood, thus doubling the number of elementary failure events to assess.

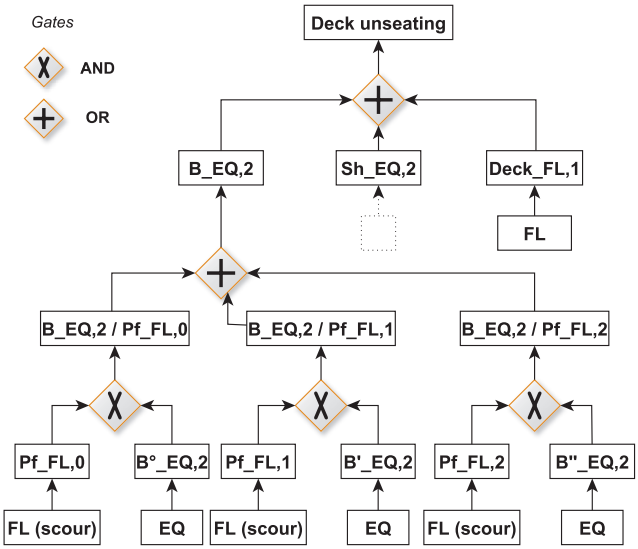

Figure 4: Fault-tree analysis for deck unseating, with the bearing failure event expanded in order to show the joint effects of earthquake and scour events.

6. MULTI-HAZARD FRAGILITY FUNCTIONS

Once the component fragility curves and the system damage states have been fully described, it is possible to derive system-level fragility functions that are able to account for the joint effect of the different loading mechanisms: since hazard-specific fragility curves from previous sections are expressed with either flow discharge Q (i.e. fluvial flood) or PGA (i.e. earthquake and ground failure), then it is possible to derive a fragility surface that expresses the damage failure with respect to two statistically independent intensity measures.

The fault-tree analysis in Figure 4 for the deck unseating event may be translated into a Bayesian Network formulation (see Figure 5): this enables to clearly identify the potential common cause failures induced by the hazard types. While the source events (e.g. EQ or FL) are present at multiple locations in the fault-tree, they are only represented once in the Bayesian Network, thus fully emphasizing the statistical dependency between the different failure events.

Correlations between failure events can then be approximated with a Dunnett-Sobel class of Gaussian random variables, as proposed by Song and Kang (2009): for each component *i*, the standard-

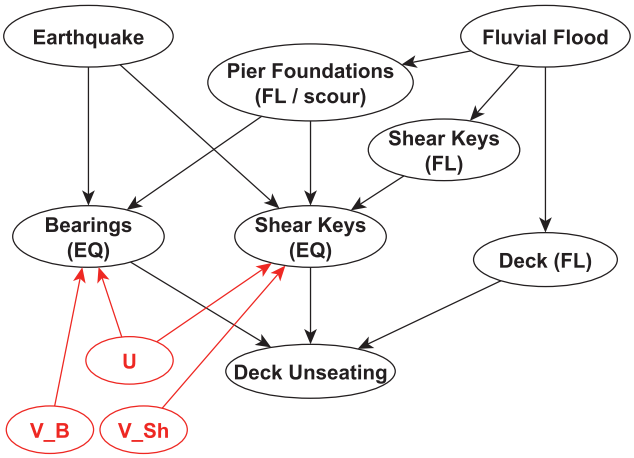

Figure 5: Bayesian Network for deck unseating (SDS3). Dunnett-Sobel variables are represented in red.

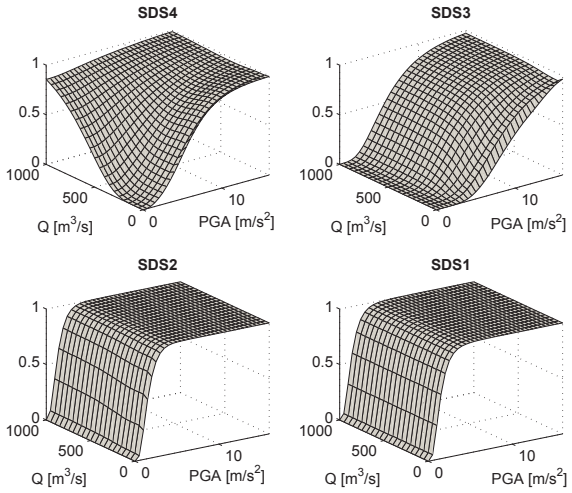

Figure 6: Multi-hazard fragility functions for the four system damage states, expressed as a function of Q and PGA.

ized safety factor Z_i (i.e. ratio of demand over capacity) can be expressed as a combination of random variables such as $Z_i = \sqrt{1-t^2} \cdot V_i + t_i \cdot U$, where the t_is have to be optimized by fitting the correlation matrix of Z_i.

Numerical seismic analysis of the bridge system enables to obtain a straightforward correlation matrix of the component responses, however this is not the case for floods and ground failures. It can however be assumed that flood- and earthquake-related failures are statistically independent, therefore a correlation factor of 0 is used between the different hazard types. The random variable representing the correlation between events has to be sampled over the whole support of the standard Gaussian distribution, which requires numerous assessments of the Bayesian Network: finally, the fragility surfaces for SDS1 to 4 are displayed in Figure 6. A cumulative representation of the damage probabilities has been chosen, however it can be seen that the definition of the four SDSs does not follow a strictly hierarchical model (e.g. the probability of reaching SDS4 is higher than the probability of reaching SDS1 for some combinations of Q and PGA).

It can be seen that the effect of fluvial flood is mainly significant for heavier system damage states, such as deck unseating or full collapse: for these damage states, it has been observed that the effect of scour or shear key removal has the most influence on the seismic response of the other bridge components. Finally, it can checked that the obtained fragility functions are consistent with the three multi-hazard scenarios that have been previously defined: if the loading history on the system is respected, the cumulative damages can be quantified for the various configurations.

7. CONCLUSIONS

This paper has shown through an elaborate example that multi-hazard fragility functions can be assembled from hazard-specific fragility curves and a corresponding Bayesian Network formulation. It should be noted that this framework allows to treat component fragility curves that have been derived through various techniques (e.g. empirical, analytical, judgement-based, with plain Monte Carlo or MFOSM methods), which are usually inherent to each hazard type. Limited knowledge on a given quantitative fragility curve could also be addressed by assigning upper and lower bound to the damage probabilities and analysing their effects on the system-level fragility functions.

Finally, this study has assumed that all pier foundations or all shear keys are in the same damage state (i.e. correlation factor of 1) due to fluvial flood, while there could actually be many configurations where only a few components have failed at the same time. Accounting for this level of de-

tail would lead to an almost intractable number of damage configurations, while the fragility functions presented here are already based on a large amount of damage-dependent fragility curves (e.g. assembly of 65 component fragility curves for SDS2). Such difficulties are mainly due to the nature of the seismic response of a structural system, where any component may have an effect on the behaviour of the other components, and reciprocally. The use of meta-models or surface responses could be a reasonable compromise to adjust the intact-state fragility curves, depending on which components have been previously damaged.

8. REFERENCES

Alipour, A. and Shafei, B. (2012). "Performance assessment of highway bridges under earthquake and scour effects." *15th World Conference on Earthquake Engineering*, Lisbon, Portugal.

Alipour, A., Shafei, B., and Shinozuka, M. (2013). "Reliability-Based Calibration of Load and Resistance Factors for Design of RC Bridges under Multiple Extreme Events: Scour and Earthquake." *Journal of Bridge Engineering*, 18, 362–371.

Gehl, P. and D'Ayala, D. (2014). "Developing fragility curves for roadway bridges using system reliability and support vector machines." *2nd European Conference on Earthquake Engineering and Seismology*, Istanbul, Turkey.

Hassan, A. M. and Wolff, T. F. (1999). "Search algorithm for minimum reliability index of earth slopes." *Journal of Geotechnical and Geoenvironmental Engineering*, 125, 301–308.

Kameshwar, S. and Padgett, J. E. (2014). "Multi-hazard risk assessment of highway bridges subjected to earthquake and hurricane hazards." *Engineering Structures*, 78, 154–166.

Kaynia, A. M., Johansson, J., Argydouris, S., and Pitilakis, K. (2012). "Fragility functions for roadway system elements." *Report no.*, SYNER-G Project Deliverable D3.7.

Lee, G. C. and Sternberg, E. (2008). "A new system for preventing bridge collapses." *Issues in Science and Technology*, 24(3).

Liang, Z. and Lee, G. C. (2013). "Bridge pier failure probabilities under combined hazard effects of scour, truck and earthquake. Part II: failure probabilities." *Earthquake Engineering and Engineering Vibration*, 12(2), 241–250.

Marzocchi, W., Garcia-Aristizabal, A., Gasparini, P., Mastellone, M. L., and Di Ruocco, A. (2012). "Basic principles of multi-risk assessment: a case study in Italy." *Natural Hazards*, 62, 551–573.

Nielson, B. G. (2005). "Analytical fragility curves for highway bridges in moderate seismic zones." Ph.D. thesis, Georgia Institute of Technology, Atlanta, Georgia.

Padgett, J. E., DesRoches, R., Nielson, B. G., Yashinsky, M., Kwon, O. S., Burdette, N., and Tavera, E. (2008). "Bridge damage and repair costs from hurricane katrina." *Journal of Bridge Engineering*, 13, 6–14.

Prasad, G. G. and Banerjee, S. (2013). "The impact of flood-induced scour on seismic fragility characteristics of bridges." *Journal of Earthquake Engineering*, 17, 803–828.

Puppala, A. J., Saride, S., Archeewa, E., Hoyos, L. R., and Nazarian, S. (2009). "Recommendations for design, construction and maintenance of brdige approach slabs: synthesis report." *Report No. FHWA/TX-09/0-6022-1*, Texas Department of Transportation, Arlington, Texas, USA.

Richardson, E. V. and Davis, S. R. (1995). "Evaluating scour at bridges." *Report No. FHWA-IP-90-017*, Federal Highway Administration, Washington, DC, USA.

Sharma, S. and Mohan, S. B. (2011). "Status of bridge failures in the United States (1800-2009)." 13.

Song, J. and Kang, W. H. (2009). "System reliability and sensitivity under statistical dependence by matrix-based system reliability method." *Structural Safety*, 31, 148–156.

Wu, X. Z. (2013). "Probabilistic slope stability analysis by a copula-based sampling method." *Computers and Geosciences*, 17, 739–755.

Wu, X. Z. (2014). "Development of fragility functions for slope instability analysis." *Landslides*, in press.